IEEE Photonics Journal
An IEEE Photonics Society Publication

Open Access

Wavelength Switchable Mode-Locked Fiber Laser With Tapered Two-Mode Fiber

Volume 11, Number 5, October 2019

Liqin Xie
Fang Fang
Bing Sun
Mengmeng Chen
Zuxing Zhang

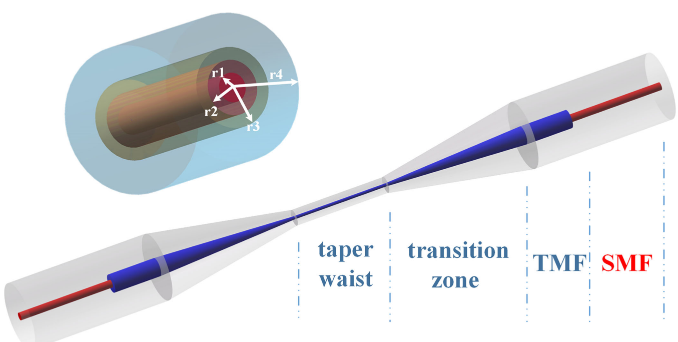

DOI: 10.1109/JPHOT.2019.2938780

IEEE photonics SOCIETY

IEEE

Wavelength Switchable Mode-Locked Fiber Laser With Tapered Two-Mode Fiber

Liqin Xie,[1] **Fang Fang,**[1] **Bing Sun**,[1] **Mengmeng Chen,**[2] **and Zuxing Zhang** [1]

[1]Advanced Photonic Technology Lab, College of Electronic and Optical Engineering & Microelectronics College, Nanjing University of Posts and Telecommunications, Nanjing 210023, China
[2]School of Electronic Engineering, Nanjing Xiaozhuang University, Nanjing 211171, China

DOI:10.1109/JPHOT.2019.2938780

Manuscript received July 21, 2019; revised August 21, 2019; accepted August 28, 2019. Date of publication August 30, 2019; date of current version September 19, 2019. This work was supported in part by the Natural Science Foundation of Jiangsu Province under Grant BK20161521; in part by Postgraduate Research & Practice Innovation Program of Jiangsu Province SJKY19_0819; in part by Six Talent Peaks Project in Jiangsu Province 2015-XCL-023; in part by Jiangsu provincial department of education 19KJB510005; and in part by Nanjing University of Posts and Telecommunications Talents NY214002 and NY215002. Corresponding authors: Zuxing Zhang and Mengmeng Chen (e-mail: zxzhang@njupt.edu.cn; chenmm@njxzc.edu.cn).

Abstract: We propose and demonstrate a wavelength switchable mode-locked Erbium-doped fiber laser with carbon nanotubes for mode-locking and a tapered two-mode fiber (TTMF) based filter for wavelength selection. The TTMF based filter constructed with single-mode fiber-TTMF-single-mode fiber configuration, features smooth interference spectrum. It is attributed to that only two modes are involved into the interference in the specially designed TTMF, which is confirmed by both simulations and experiments. Moreover, the free spectral range (FSR) of the TTMF based filter can be arbitrarily chosen by controlling the taper diameter. Depending on the FSR of the TTMF based filter, the central wavelengths of the mode-locking operation of the Erbium-doped fiber laser based on carbon nanotubes can be switched between two wavelengths with FSR of 8.5 nm and three wavelengths with FSR of 3.1 nm, respectively. This fiber laser is flexible source for various applications.

Index Terms: Tapered two-mode fiber, wavelength switchable laser, mode-locked fiber laser.

1. Introduction

Nowadays, with the rapid increase of communication capacity, modern optical fiber communication systems are required to increase and flexibly control the number of channels [1], [2]. Wavelength switchable laser can meet the requirement of flexible wavelength choice, which is equivalent to multiple available lasers with different emission wavelengths. Thus, compared with single wavelength laser, wavelength switchable laser is more convenient and cost efficient. Besides the wavelength switchable continuous-wave (CW) lasers [3]–[5], the wavelength switchable mode-locked lasers generating high-power and ultra-short optical pulses are desirable light sources for time/wavelength division multiplexing optical communication systems [6], [7]. Furthermore, the high-intensity pulsed beam can result in nonlinear effects and photo-luminescence effects, thus it can also be widely used in spectroscopy [8], optical signal processing [9] and so on.

Up to now, a variety of switchable fiber lasers have been developed with different filters. In 2008, Tran *et al.* proposed a switchable multi-wavelength Erbium-doped fiber laser based on a

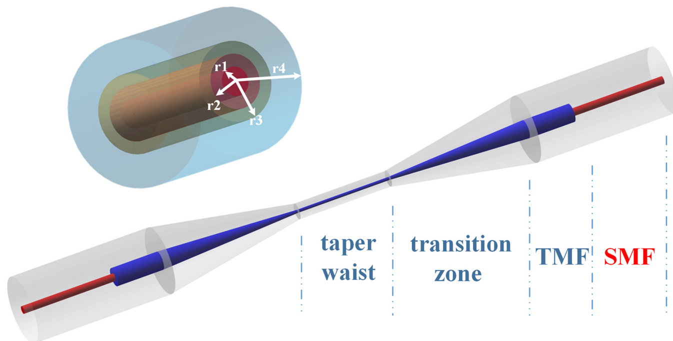

Fig. 1. Schematic structure of SMF-TTMF-SMF filter.

nonlinear optical loop mirror incorporating multiple fiber Bragg gratings [10]. In 2010, Luo *et al.* proposed a switchable multi-wavelength passively mode-locked fiber laser with a channel spacing of 3.65 nm in a 3-dB bandwidth by exploiting a polarization maintaining fiber (PMF) filter [11]. In 2011, Zhu *et al.* used a phase-shifted long-period fiber grating (PS-LPFG) as a spectral filter in the laser cavity, achieving a stable and switchable dual-wavelength mode-locked operation [12]. In 2016, Cheng *et al.* used two Sagnac loops with a chirped fiber grating and polarization-maintaining fiber as comb filters to excite multi-wavelength output [13]. In 2018, Zhou *et al.* proposed a switchable multi-wavelength erbium-doped fiber laser based on a four-mode fiber Bragg grating (FBG), which can support four linearly polarized modes around 1550 nm [14]. In 2019, Zhao *et al.* employed a phase-shifted fiber Bragg grating (PS-FBG) combined with Sagnac loop structure to filter and the output wavelength range of fiber laser is 1556.128–1556.384 nm [15]. Overall, fiber grating, PMF and their combination are commonly used methods for switchable wavelength generation [16]–[18]. However, fiber grating involves complicated fabrication and lacks wavelength flexibility, while the use of PMF may introduces excess birefringence dispersion. It is well known that tapered fiber can be used for various optical fiber devices because of its characteristics, such as high nonlinearity, strong evanescent field [19]. The other great advantage of the tapered fiber is compatible and integrated with fiber-based system, through fiber fusion with low loss [20].

In this paper, we demonstrate a wavelength switchable passively mode-locked fiber laser incorporating carbon nanotubes as mode-locker and TTMF based filter as wavelength selector. The used TTMF based filter is constructed with single-mode fiber-TTMF- single-mode fiber configuration, which features smooth interference spectrum. Our simulations and experiments have sufficiently testified that only two modes involved into the interference in the TTMF leads to smooth interference spectrum, and the manipulation of the taper diameter bring about the optional free spectral range (FSR) of the TTMF based filter. In laser experiments, the mode-locked fiber lasers with central wavelengths switchable between two wavelengths with FSR of 8.5 nm and three wavelengths with FSR of 3.1 nm, have been realized depending on the FSR of the TTMF based filter, respectively. This fiber laser may find great application in fields demanding flexible source.

2. Characteristics of TTMF

2.1 Fabrication of TTMF

TTMF based filter, as schematically shown in Fig. 1, is constructed by incorporating a section of TTMF between two single-mode fibers (SMFs). The core radius (r1), the radius of second layer (r2), the radius of third layer (r3), the radius of the outer cladding (r4) of the used TMF are 7 μm, 13 μm, 19 μm and 62.5 μm, respectively. Their refractive indexes are n1 (1.4485), n2 (1.444), n3 (1.435336) and n4 (1.444), respectively. The TMF can support fundamental mode (LP01) and the second-order mode (LP11). In SMF part, the fiber only transmits the fundamental modes (LP01). As the diameter of TTMF gradually decreases to the size of waist diameter, the fiber core almost disappears. In this

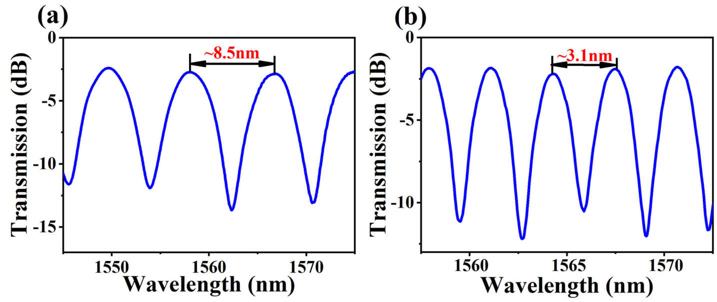

Fig. 2. Transmission spectra of the TTMF structures with different FSR.

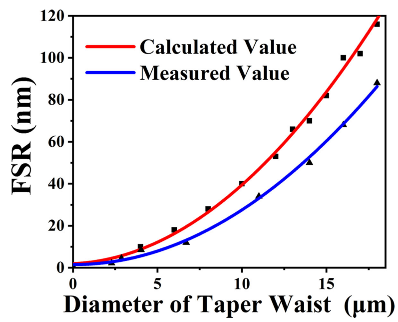

Fig. 3. FSR of the TTMF based filter versus taper diameter from simulation calculation (red line) and experiment measurement (blue line).

case, LP01 mode and LP11 mode becomes guided-cladding modes [21]. Furthermore, these two modes combined at the output SMF results with suitable interference spectrum.

Regarding the fabrication of TTMF based filter, firstly the SMF-TMF-SMF structure is prepared, and then the TMF part is tapered through the flame tapering method. The tapered fiber includes two parts, which are transition zone and taper waist. The diameter of the taper waist portion is uniform, while the transition zone (connecting the taper waist portion and the unstretched portion) is nonuniform. After tapering, the structure is solidified and encapsulated with UV adhesive to ensure the wavelength stability and application convenience.

In our experiments, we prepared two TTMFs, and the length of the first TTMF's transition portion and waist portion are shorter than that of the second one. A broadband light source is used to characterize the TTMF based filter, and an optical spectrum analyzer is used to measure the transmission spectrum. Fig. 2 shows the transmission spectra measured for two TTMF based filters with different FSR. From Fig. 2, the FSRs are 8.5 nm and 3.1 nm, respectively, and the corresponding insertion loss of both filters is about 2.5 dB.

2.2 Characteristics of TTMF

In order to explore the characteristics of the TTMF, we characterized them from the two aspects of both simulation and experiment. On the one hand, the influence of the morphology of the taper region on the FSR of the tapered fiber based filter can be calculated by using the finite difference beam propagation method. In the process of simulation, the length of transition zone is kept at 3.5 mm and the length of taper waist portion is 5.5 mm. By changing the diameter of taper waist portion, the FSR corresponding to different taper waist diameters can be obtained. It can be seen from the red curve in Fig. 3 that the FSR of TTMF increases with the increase of taper waist diameter. On the other hand, the diameter of the taper waist portion can be changed by changing the time of flame tapering. So, we prepare several different TTMF samples. The taper waist diameters of the

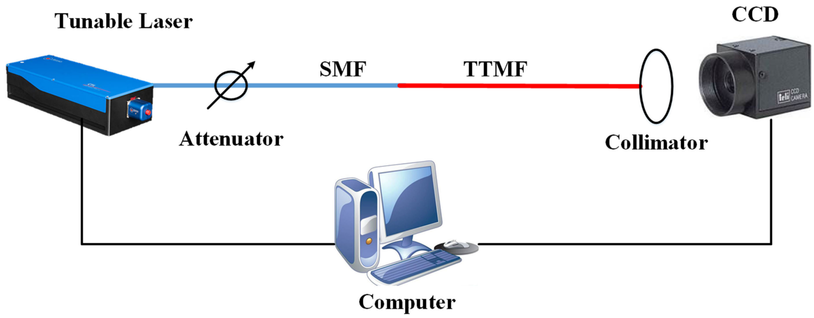

Fig. 4. Schematic of S^2 analysis method.

TTMFs are measured by the optical microscope, and the FSRs are measured by the spectrometer. By fitting these data, the blue curve in Fig. 3 can be drawn. By comparing the two curves of simulation calculation and experimental measurement, it can be seen that the variation trend of the simulation result is consistent with that of the experimental measurement result, and the conclusion is that the larger the diameter of taper waist, the wider the FSR of the TTMF based filter. The discrepancy of the specific values between the simulation and measurement is due to the selection of parameter value for the simulation.

2.3 Mode Analysis by Spatially and Spectrally Resolved Imaging Technology

Spatially and Spectrally (S^2) resolved imaging technology is a method for measuring the mode characteristics of optical fibers proposed by J. W. Henderson *et al.* in 2008, as large mode field fiber is increasingly used in fiber lasers and fiber laser amplifiers. Since the group velocity of optical signals in fiber will be different due to different modes, beat frequency signals between different modes will be generated. Such beat frequency will lead to coupling between different modes and multiple path interference (MPI) [22] in the few mode fibers. Because of the coupling phenomenon between modes, part of the energy in the fundamental mode will be transferred into the higher-order mode. By analyzing the beat frequency signal of the fiber, the coupling phenomenon of different modes in the fiber can be clearly comprehended [23].

The S^2 analysis uses the spectrum of optical fiber transmission and the spatial superposition of fundamental mode and higher-order mode during the transmission process to analyze the characteristics of the few mode fibers. There are different modes in the few mode fiber, the propagation speed of different modes in the fiber will be slightly different, thus the interference between modes will occur in the propagation process. By analyzing the spatial and spectral characteristics of the transfer mode in the optical fiber, we can obtain the parameters related to the mode of the optical fiber accurately. To verify the claim that adiabatic taper profiles of the two-mode fiber only allow excitation and transmission of LP01 mode and LP11 mode, the S^2 analysis method is used to investigate the transmission mode in the TTMF.

It can be seen from Fig. 4 that the tunable wavelength laser light emitted by the tunable laser firstly passes through the optical fiber patch cord, and then is injected into the TTMF fixed on the collimator. The laser light transmitting through the fiber is imprinted on the photosensitive surface of the CCD, and the data of the mode field distribution can be collected by CCD. Since the spectrum obtained from untapered TMF has no interference effect, that is, the high-order mode is extremely weak, we infer that the generation of high-order mode is mainly caused by taper waist portion. Therefore, in the process of the S^2 analysis experiment, the TTMF is cut in the middle to explore and obtain the propagation mode data in the taper waist portion.

Fig. 5(a) shows the spot of light emitted from the middle of the TTMF, recorded by the CCD. It is supposed to be a superposition of high-order modes with the fundamental mode, instead of a regular fundamental mode. Fig. 5(b) is the corresponding spatial frequency spectrum of TTMF, obtained by using S^2 resolved imaging technology. It can be seen from the diagram that LP01 and

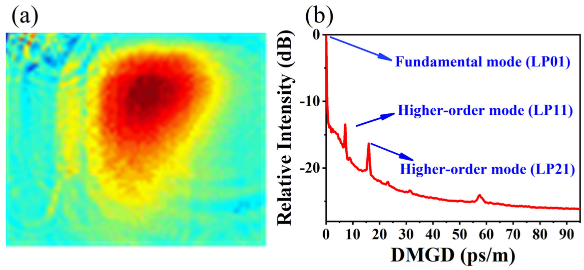

Fig. 5. (a) Spot of light emitted from the middle of the TTMF recorded by the CCD, (b) corresponding spatial frequency spectrum.

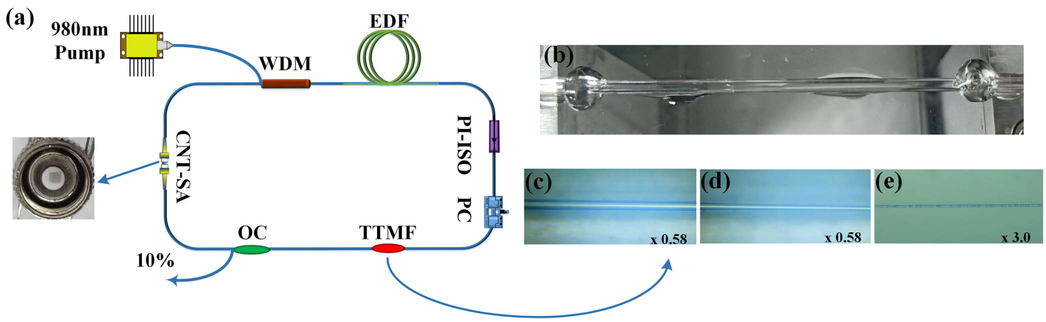

Fig. 6. (a) Schematic of wavelength switchable fiber laser with TTMF based filter, microscopic images of (b) the whole TTMF, (c) unstretched portion, (d) transition zone, (e) taper waist portion.

LP11 modes account for a large proportion. The result is consistent with our theoretical assumption and simulations: the core almost disappears, and the cladding becomes a new core, LP01 and LP11 modes become waveguide cladding modes, as the diameter of TTMF gradually decreases. The two kinds of modes are combined to obtain a smooth interference spectrum.

3. Experimental Setup

The schematic of wavelength switchable mode-locked fiber laser with TTMF based filter is shown in Fig. 6. It is a ring cavity configuration that includes 1.4 m erbium-doped fiber (EDF) with a dispersion parameter D of −48 ps/(nm·km) at 1550 nm and a 5.6 m SMF with a dispersion parameter D of 17 ps/(nm·km), respectively. The total cavity length is 7 m and the net dispersion is -0.042 ps^2. The carbon nanotube-saturable absorber (CNT-SA) (microscopic image shown in left inset of Fig. 6(a)) is considered as a mode-locker and TTMF based filter (microscopic images shown in Figs. 6(b–e)) is used to generate wavelength switchable phenomenon. A polarization independent isolator (PI-ISO) is inserted into the cavity to ensure unidirectional transmission in the cavity. A PC is used to control the polarization state of light in the cavity. The fiber laser is pumped by the 980 nm laser diode through a 980 nm/1550 nm wavelength division multiplexing coupler (WDM). A 90/10 optical coupler (OC) is used to extract 10% energy from the cavity for signal detection.

4. Results and Discussions

4.1 Wavelength Switchable Mode-Locked Fiber Laser Incorporating TTMF With FSR of 8.5 nm

When the pumping power increases to 120 mw, the laser began to generate mode-locked pulses. Adjusting the PC, the wavelength can be switched at 1560.0 nm and 1568.5 nm. As shown in

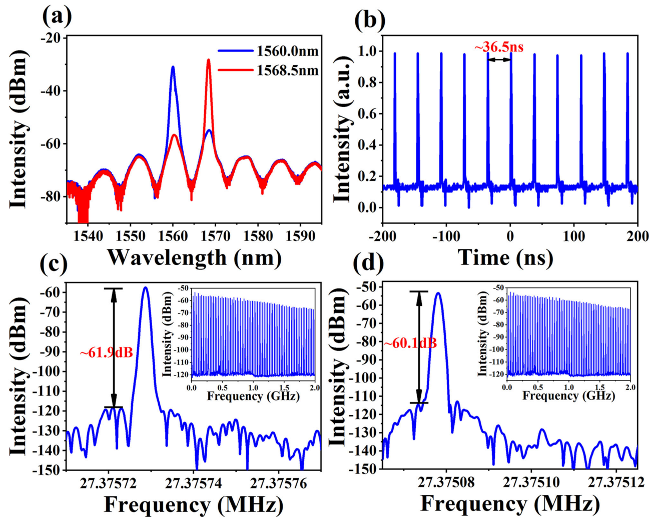

Fig. 7. (a) Output optical spectra, (b) pulse train, (c) RF spectrum of pulses at 1560.0 nm, (d) RF spectrum of pulses at 1568.5 nm for wavelength switchable mode-locked fiber laser incorporating TTMF with FSR of 8.5 nm.

Fig. 7(a), the central wavelengths differ by 8.5 nm, corresponding to the FSR of the TTMF. As depicted in Fig. 7(b), the pulse period is 36.5 ns and the repetition frequency is 27.37 MHz. As shown in Fig. 7(c) and Fig. 7(d), the RF spectrums display that the signal to noise ratio (SNR) at 27.376 MHz is 61.9 dB and the SNR at 27.375 MHz is 60.1 dB, which further prove that the mode-locked fiber laser operates in single pulse state. The value of SNR is rather large, so the mode-locking state is stable. The repetition rate difference can be calculated as the formula mentioned in [25]:

$$\Delta f = \Delta\lambda L D / T^2 \tag{1}$$

In this experiment, the wavelength switchable mode-locked fiber laser has L $\approx$ 7 m, D $\approx$ 22.2 ps/(nm·km) and T $\approx$ 36.5 ns. The calculated fundamental repetition rate difference is $\sim$991 Hz, which is almost identical to the measured result, 650 Hz. When the pump power increases to 135 mw, the mode-locked phenomenon becomes unstable because of the saturation of CNT-SA. If the power continues to increase, it will lead to the damage of CNT-SA.

4.2 Wavelength Switchable Mode-Locked Fiber Laser Incorporating TTMF With FSR of 3.1 nm

Benefiting from the FSR controllability, a TTMF based filter with FSR of 3.1 nm has also been fabricated, replacing the previous one for laser experiments. For this case, the mode-locked threshold power of the laser is 106 mw. As depicted in Fig. 8(a), the central wavelengths can be switched between three different wavelengths, which are 1561.8 nm, 1564.9 nm, 1568.0 nm, respectively. The central wavelengths differ by 3.1 nm, corresponding to the FSR of the TTMF. Fig. 8(b) shows that the pulse period is 35 ns and the repetition frequency is 28.67 MHz. The SNR at 28.67 MHz is 63.4 dB, as depicted in Fig. 8(c). Fig. 8(d) shows the slope efficiency of the laser. It can be seen from the diagram that the slope efficiency is 0.3%. When the pump power increases to 123 mw, the mode-locked phenomenon becomes unstable.

From the experimental results above, we can conclude that when FSR is 8.5 nm, the central wavelength of the laser can be switched between two different wavelengths. As FSR is decreased to 3.1 nm, the central wavelength of the laser can be changed between three different wavelengths. By changing TTMF structures with different FSR, we can find out that the smaller the FSR, the

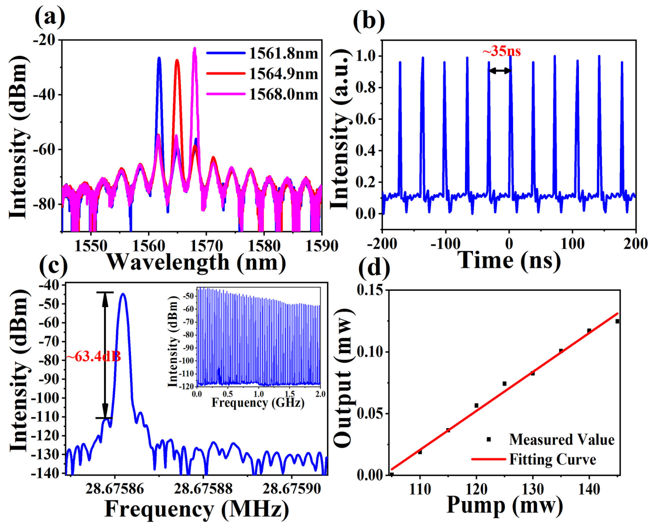

Fig. 8. (a) Output optical spectra, (b) pulse train, (c) RF spectrum, and (d) slope efficiency for wavelength switchable mode-locked fiber laser incorporating TTMF with FSR of 3.1 nm.

more switchable wavelengths can be obtained. Therefore, as long as the FSR is small enough, the laser may be switched between more wavelengths.

5. Conclusions

We have proposed and demonstrated a switchable mode-locked fiber laser based on TTMF and CNT-SA to generate switchable wavelength mode-locked pulse output. The TTMF based filter constructed with single-mode fiber-TTMF-single-mode fiber configuration is a novel comb filter, which is used to achieve switchable wavelengths. Our simulations and experiments have sufficiently testified that only two modes involved into the interference in the TTMF leads to smooth interference spectrum, and the manipulation of the taper diameter bring about the optional FSR of the TTMF based filter. Compared with other filters, TTMF based filter has many advantages such as compatibility with fiber-based system, low insertion loss, and manipulable FSR. The mode-locked fiber lasers with central wavelengths switchable between several wavelengths with different FSR have been realized depending on the FSR of the TTMF based filter. It has very important application prospects in the fields of optical sensing, optical measurement, optical signal processing and wavelength division multiplexing optical transmission systems.

References

[1] P. C. Peng, R. K. Shiu, M. A. Bitew, T. L. Chang, C. H. Lai, and J. I. Junior, "A 12 GHz wavelength spacing multi-wavelength laser source for wireless communication systems," *Opt. Laser Technol.*, vol. 93, pp. 175–179, 2017.

[2] P. Marin-Palomo *et al.*, "Microresonator-based solitons for massively parallel coherent optical communications," *Nature*, vol. 546, no. 7657, pp. 175–179, 2017.

[3] X. Luo, T. H. Tuan, T. S. Saini, H. P. T. Nguyen, T. Suzuki, and Y. Ohishi, "Multi-wavelength Erbium-doped fiber laser with tunable wavelength spacing," in *Proc. Int. Joint Conf. E-Business Telecommun.*, 2018, vol. 1, pp. 407–411.

[4] Q. Fu *et al.*, "Multi-wavelength lasing oscillation based on polarization hole burning effect in an Erbium-doped fiber laser," in *Proc. 16th Int. Conf. Opt. Commun. Netw.*, 2017, vol. 1, pp. 1–3.

[5] K. Y. Lau, M. H. A. Bakar, A. R. M. Zain, A. F. Abas, M. T. Alresheedi, and M. A. Mahdi, "Stable multi-wavelength erbium-doped fiber laser assisted by graphene/PMMA thin film," *Opt. Laser Technol.*, vol. 105, pp. 129–134, 2018.

[6] D. Li *et al.*, "Wavelength and pulse duration tunable ultrafast fiber laser mode-locked with carbon nanotubes," *Sci. Rep.*, vol. 8, no. 2738, pp. 1–8, 2018.

[7] X. X. Jin *et al.*, "102 fs pulse generation from a long-term stable, inkjet-printed black phosphorus-mode-locked fiber laser," *Opt. Exp.*, vol. 26, no. 10, pp. 12506–12513, 2018.

[8] R. L. Swofford and A. C. Albrecht, "Nonlinear spectroscopy," *Annu. Rev. Phys. Chem.*, vol. 29, no. 1, pp. 421–440, 1978.
[9] Z. Y. Yan *et al.*, "Widely tunable Tm-doped mode-locked all-fiber laser," *Sci. Rep.*, vol. 6, no. 27245, pp. 1–7, 2016.
[10] T. V. A. Tran, K. Lee, and S. B. Lee, "Switchable multiwavelength erbium doped fiber laser based on a nonlinear optical loop mirror incorporating multiple fiber Bragg gratings," *Opt. Exp.*, vol. 16, no. 3, pp. 1460–1465, 2008.
[11] Z. C. Luo, A. P. Luo, and W. C. Xu, "Tunable and switchable multiwavelength passively mode-locked fiber laser based on SESAM and inline birefringence comb filter," *IEEE Photon. J.*, vol. 3, no. 1, pp. 64–70, Feb. 2011.
[12] X. J. Zhu, C. H. Wang, S. X. Liu, D. F. Hu, J. J. Wang, and C. Y. Zhu, "Switchable dual-wavelength and passively mode-locked all-normal-dispersion Yb-doped fiber lasers," *IEEE Photon. Technol. Lett.*, vol. 23, no. 14, pp. 956–958, Jul. 2011.
[13] J. Q. Cheng, W. C. Chen, and G. J. Chen, "Switchable quadruple-wavelength Erbium-doped fiber laser based on a chirped fiber grating and polarization-maintaining fiber," *Opt. Laser Technol.*, vol. 78, pp. 71–73, 2016.
[14] Y. Zhou, P. Y. Gao, X. Zhang, P. Wang, L. Chen, and W. Q. Gao, "Switchable multi-wavelength erbium-doped fiber laser based on a four-mode FBG," *Chin. Opt. Lett.*, vol. 17, no. 1, 2019, Art. no. 010604.
[15] X. L. Zhao, F. Luo, Y. M. Zhang, F. Y. Meng, and M. L. Dong, "A switchable dual-wavelength fiber laser based on phase-shifted fiber Bragg grating combined with Sagnac loop," *Optoelectron. Lett.*, vol. 15, no. 2, pp. 122–126, 2019.
[16] J. M. Liu, Y. Chen, Y. Li, H. Zhang, S. Q. Zheng, and S. X. Xu, "Switchable dual-wavelength Q-switched fiber laser using multilayer black phosphorus as a saturable absorber," *Photon. Res.*, vol. 6, no. 3, pp. 198–203, 2018.
[17] W. He, G. S. Zhong, L. Q. Zhu, M. L. Dong, and G. H. Chen, "Wavelength-switchable erbium-doped fiber laser based on femtosecond FBG inscribed on fiber core and cladding through the coating," *Laser Phys. Lett.*, vol. 16, no. 5, 2019, Art. no. 055104.
[18] X. L. Zhao, M. L. Dong, Y. M. Zhang, F. Luo, and L. Q. Zhu, "Switchable multi-wavelength and tunable wavelength spacing erbium-doped fiber laser based on a phase-shifted fiber Bragg grating combined with a Mach-Zehnder interferometer," *Opt. Laser Technol.*, vol. 112, pp. 500–507, 2019.
[19] Q. Y. Song, G. X. Chen, and K. Tian, "Tunable fiber lasers based on tapered fiber," *Laser Optoelectron. Prog.*, vol. 628, no. 5, pp. 286–291, 2018.
[20] D. Türke, J. Teipel, and H. Giessen, "Manipulation of supercontinuum generation by stimulated cascaded four-wave mixing in tapered fibers," *Appl. Phys. B*, vol. 92, no. 2, pp. 159–163, 2008.
[21] B. Sun, F. Fang, Z. X. Zhang, J. Xu, and L. Zhang, "High-sensitivity and low-temperature magnetic field sensor based on tapered two-mode fiber interference," *Opt. Lett.*, vol. 43, no. 6, pp. 1311–1314, 2018.
[22] S. Ramachandran, S. Ghalmi, and J. Bromage, "Evolution and systems impact of coherent distributed multipath interference," *IEEE Photon. Technol. Lett.*, vol. 17, no. 1, pp. 238–240, Jan. 2005.
[23] J. W. Nicholson, A. D. Yablon, S. Ramachandran, and S. Ghalmi, "Spatially and spectrally resolved imaging of modal content in large-mode-area fibers," *Opt. Exp.*, vol. 16, no. 10, pp. 7233–7243, 2008.
[24] S. Celaschi and G. N. Malheiros-Silveira, "High-resolution and low-loss all-fiber spectral filters based on biconic tapers," *J. Lightw. Technol.*, vol. 35, no. 24, pp. 5381–5384, Dec. 2017.
[25] X. Luo, T. H. Tuan, T. S. Saini, H. P. T. Nguyen, T. Suzuki, and Y. Ohishi, "Tunable and switchable all-fiber dual-wavelength mode locked laser based on Lyot filtering effect," *Opt. Exp.*, vol. 27, no. 10, pp. 14635–14647, 2019.